Journal of the American College of Cardiology
© 2009 by the American College of Cardiology Foundation
Published by Elsevier Inc.

Vol. 54, No. 15, 2009
ISSN 0735-1097/09/$36.00
doi:10.1016/j.jacc.2009.04.094

STATE-OF-THE-ART PAPER

The Role of Cardiovascular Magnetic Resonance Imaging in Heart Failure

Theodoros D. Karamitsos, MD, PHD,* Jane M. Francis, DCC(R), DNM,* Saul Myerson, MD,* Joseph B. Selvanayagam, MBBS, DPHIL,† Stefan Neubauer, MD*

Oxford, United Kingdom; and Adelaide, Australia

Noninvasive imaging plays a central role in the diagnosis of heart failure, assessment of prognosis, and monitoring of therapy. Cardiovascular magnetic resonance (CMR) offers a comprehensive assessment of heart failure patients and is now the gold standard imaging technique to assess myocardial anatomy, regional and global function, and viability. Furthermore, it allows assessment of perfusion and acute tissue injury (edema and necrosis), whereas in nonischemic heart failure, fibrosis, infiltration, and iron overload can be detected. The information derived from CMR often reveals the underlying etiology of heart failure, and its high measurement accuracy makes it an ideal technique for monitoring disease progression and the effects of treatment. Evidence on the prognostic value of CMR-derived parameters in heart failure is rapidly emerging. This review summarizes the advantages of CMR for patients with heart failure and its important role in key areas. (J Am Coll Cardiol 2009; 54:1407–24) © 2009 by the American College of Cardiology Foundation

Heart failure (HF) is associated with significant morbidity, mortality, and financial burden to health care services (1). In the U.S., around 5,700,000 people, representing 2.5% of Americans older than 20 years of age, have been diagnosed with this condition (2). The aging of the population and the improved prognosis of patients with acute coronary events further fuel the HF epidemic. Consequently, hospital discharges in the U.S. for HF increased from 877,000 in 1996 to 1,106,000 in 2006 (13% increase) (2).

The early diagnosis and identification of the underlying etiology of HF is of paramount importance, because although the general treatment is common to many patients, some causes require specific treatment and may be correctable. Noninvasive imaging plays a central role in the diagnosis of HF, the assessment of prognosis, and monitoring of therapy. The recently updated American College of Cardiology/American Heart Association guidelines (3) note that when imaging techniques are used to assess patients with HF, 3 fundamental questions must be addressed: 1) Is the left ventricular (LV) ejection fraction preserved or reduced? 2) Is the structure of the LV normal or abnormal? 3) Are there other structural abnormalities such as valvular, pericardial, or right ventricular (RV) abnormalities that could account for the clinical presentation? Two-dimensional echocardiography is currently the imaging modality most commonly used to answer these questions, and will remain so for the foreseeable future. It provides a good general assessment of LV function but is limited in patients with poor acoustic windows, it requires geometric assumptions in quantifying global LV systolic function, and its ability to provide specific tissue characterization is modest.

Cardiovascular magnetic resonance (CMR) is a rapidly evolving technology that is increasingly being used for the noninvasive imaging of the expanding HF population. In this review we discuss: 1) how CMR works; 2) what type of information CMR can provide in patients with HF, with particular emphasis on its ability to accurately subclassify such patients; and 3) what the expanding role of CMR is for prognostic evaluation in the HF population.

How Does CMR Work?

Currently, CMR is generally performed at a magnetic field strength of 1.5-T, which is around 30,000 times stronger than the earth's magnetic field (more recently, 3.0-T magnets are increasingly being used). This powerful magnetic field is used to align the nuclear magnetization of hydrogen atoms, which are abundant in the human body. These hydrogen nuclei are then excited intermittently by pulses of radiofrequency waves (a magnetic resonance [MR] sequence), and the signal emitted from the body in return is detected with MR receiver coils. In MR imaging, signal from a given tissue (e.g., heart muscle, fat, and so on) is determined by its density of hydrogen atoms (proton density), and by 2 distinct MR relaxation parameters,

From the *University of Oxford Centre for Clinical Magnetic Resonance Research, Department of Cardiovascular Medicine, John Radcliffe Hospital, Oxford, United Kingdom; and the †Department of Cardiovascular Medicine, Flinders Medical Centre, Adelaide, Australia. Funded by the British Heart Foundation, the UK Medical Research Council, the National Institute for Health Research Biomedical Research Centre Programme, and Heart Research UK.

Manuscript received February 25, 2009; revised manuscript received April 14, 2009, accepted April 28, 2009.

JACC Vol. 54, No. 15, 2009
October 6, 2009:1407–24

Abbreviations and Acronyms

ARVC = arrhythmogenic right ventricular cardiomyopathy
CAD = coronary artery disease
CMR = cardiovascular magnetic resonance
CRT = cardiac resynchronization therapy
DCM = dilated cardiomyopathy
HCM = hypertrophic cardiomyopathy
HF = heart failure
LGE = late gadolinium enhancement
LV = left ventricular
MR = magnetic resonance
RV = right ventricular

longitudinal relaxation time (T1) and transverse relaxation time (T2). Proton density, T1, and T2 can vary substantially for different tissues, and these differences are used to generate contrast in MR images. Image contrast can also be modified by modulating the way the radiofrequency pulses are played out (the MR sequence). For example, in so-called T1-weighted images, myocardial tissue is dark, whereas fat is bright. On the other hand, T2-weighted images highlight unbound water in the myocardium and are used to show myocardial edema caused by inflammation or acute ischemia (4).

A CMR sequence consists of a series of radiofrequency pulses, magnetic gradient field switches, and timed data acquisitions, all applied in a precise order to generate the CMR image. Spin echo sequences are mainly used for anatomic imaging and tissue characterization. Gradient echo sequences show fat and blood as white and can be used to acquire cine images. The most recent standard cardiac MR sequences are steady-state free precession, which provide the best contrast between chamber blood (white) and myocardium (dark), and these are now routinely used for imaging of cardiac function. Fat suppression sequences allow signal from fat to be specifically suppressed with special pre-pulses. Several other approaches exist, and CMR sequence development is a rapidly evolving field. However, a detailed description of this is beyond the scope of this review.

To prevent artifacts from cardiac motion, most CMR images are generated with fast sequences gated to the R-wave of the electrocardiogram. Respiratory motion, another source of artifacts, is usually eliminated by acquiring CMR images in end-expiratory breath-hold.

For infarct/fibrosis imaging, intravenous gadolinium-chelated contrast agents, such as gadolinium diethylenetriamine penta-acetic acid are needed. The physiological basis of late gadolinium enhancement (LGE) is an increase in its volume of distribution within areas of scarring or fibrosis and an abnormally prolonged washout related to decreased functional capillary density in the irreversibly injured myocardium (5–8). The regional increase in extracellular volume available for gadolinium distribution produces T1 shortening, which manifests as hyperenhancement (high signal) in areas of abnormality on so-called inversion-recovery CMR images: by "nulling" the normal myocardial signal, the area of myocardial injury appears extremely bright, with high signal contrast relative to the black normal myocardium.

For perfusion imaging, the dynamic passage of a gadolinium-based contrast bolus is followed through the cardiac chambers and the myocardium. Pharmacologic vasodilation (with adenosine or dipyridamole) induces a 3- to 5-fold increase of blood flow in myocardial areas subtended by normal coronary arteries, whereas no (or only minimal) change is found in areas subtended by stenotic coronary arteries. Thus, contrast arrival in these areas is delayed, and they therefore appear hypointense (dark) compared with adjacent normal myocardium.

CMR Safety

The CMR scan subjects and operators are not exposed to ionizing radiation, and there are no known detrimental biological side effects of MR imaging if safety guidelines are followed (9). However, only trained staff should have access to the magnet room, because any iron-based item with ferromagnetic properties can be pulled into the magnet's core at high speed, potentially causing serious injury and damage. Patients with implanted electronic devices such as pacemakers or defibrillators are generally not accepted for CMR scanning (9), although this may change in the future with further technical development (MR-compatible pacemakers, and so on). Some neurological devices such as cerebrovascular clips continue to pose a problem, as do metallic objects in delicate positions, e.g., within the eye. Generally, most medical metallic implants are safe in a CMR environment, including nearly all prosthetic cardiac valves, coronary and vascular stents, and orthopedic implants. However, whenever there is uncertainty regarding a particular device or implant, its CMR safety status should be checked by referring to information provided by the manufacturer.

Gadolinium-based contrast agents have recently been linked with a rare multisystemic fibrosing disorder of unknown etiology called nephrogenic systemic fibrosis (10). The patients at risk of developing this disease are those with acute or chronic severe renal insufficiency (glomerular filtration rate <30 ml/min/1.73 m^2) or renal dysfunction caused by the hepatorenal syndrome or in the perioperative liver transplantation period (11). In the latter 2 conditions, the risk applies to any severity of renal dysfunction. At present, there is no evidence that immediate hemodialysis protects against nephrogenic systemic fibrosis. Therefore, in high-risk patients, gadolinium-based contrast media should be avoided unless the diagnostic information is essential and not available from noncontrast enhanced CMR or other imaging modalities. It should be mentioned that gadolinium-based contrast agents are not approved by the U.S. Food and Drug Administration for use in cardiac studies in the U.S.

What Are the Imaging Questions in HF That CMR Has to Answer?

There are a number of important questions that CMR has to address. For example, what is the extent of LV and RV

global and regional dysfunction and dilation, what is the underlying etiology of HF, and can modifiable components of the disease process be identified?

Unlike echocardiography, CMR has the ability to image in any desired plane and with a nearly unrestricted field of view, allowing unprecedented flexibility to evaluate abnormal cardiac and extracardiac structures. The functional information derived from cine CMR includes global LV and RV volumes and mass, without the need to make any geometrical assumptions, and therefore applies to ventricles of all sizes and shapes, even to those that have been extensively remodeled (12,13). Importantly, all major CMR techniques (e.g., volume and mass assessment with cine imaging, identification and quantification of fibrosis/scarring, quantification of valvular lesions) are not only highly accurate but also very reproducible (14–16). Moreover, the inherent 3-dimensional nature of CMR makes it particularly well suited to studying the RV, which is difficult to assess with echocardiography because of its complex and variable morphology. With regard to regional ventricular function, CMR enables the accurate identification of even subtle regional wall motion abnormalities with the use of steady-state free-precession sequences, which provide excellent delineation of the blood–myocardium interface (17). These sequences also enable the evaluation of valve structure, although valve morphology is generally better assessed by echocardiography. Although that technique is the standard tool for initial assessment and longitudinal evaluation of patients with valvular heart disease, CMR is an attractive alternative, particularly in subjects with poor acoustic windows. For flow assessment, velocity-encoding CMR sequences, which enable accurate quantitative measurements for stenotic (peak velocity and by applying the Bernoulli equation peak gradient) and regurgitant valvular lesions (regurgitant volume and fraction), are used (18). Furthermore, when a shunt is suspected, the pulmonary-to-systemic flow ratio (Q_P/Q_S) can be determined by measuring flow in the main pulmonary artery and the ascending aorta.

Specific CMR sequences (T1- or T2-weighted as described previously) can enable myocardial tissue characterization, based on the different relaxation properties of tissues such as fat, muscle, and areas of inflammation. Intracardiac thrombi can also be detected using images acquired early (1 to 3 min) after gadolinium administration with inversion recovery sequences (so-called early gadolinium imaging). Images acquired later (5 to 20 min after 0.1 to 0.2 mmol/kg gadolinium injection) using the same sequences constitute the LGE-CMR technique. The development of this technique has substantially expanded the role of CMR in the evaluation of HF patients. Viability/post-myocardial infarction scarring can be described with unprecedented resolution, and highly specific patterns of fibrosis and scarring have been described for many nonischemic cardiomyopathic processes, providing valuable diagnostic and pathophysiological insights (Fig. 1) (7,19). Furthermore, several other CMR techniques such as first-pass perfusion with or without vasodilator stress, and MR angiography are used on an individual case basis depending on the clinical history.

Nearly one-half of HF patients have abnormalities in diastolic function with preserved ejection fraction (20). CMR can assess diastolic function in several ways. In a manner analogous to echocardiography, velocity encoding CMR can measure early diastolic (E) and atrial systolic (A) peak flow velocities and E/A ratios of the mitral inflow (21). Furthermore, time–volume curves generated from retrospectively gated cine images provide indexes of global diastolic function, such as peak filling rate and time to peak filling rate (22). Magnetic resonance tagging is a sophisticated method for quantitative analysis of regional systolic and diastolic function. Selective saturation prepulses are used to superimpose a grid across the field of view. The grid lines are deformed by myocardial contraction, strain, and torsion, allowing direct quantification of myocardial deformation and strain (23). Although all of these CMR techniques provide useful information on diastolic function, they are limited by relatively complex and time-consuming post-processing compared with echocardiography, which remains the standard technique for assessment of diastolic function (24).

The ability of CMR to provide a specific diagnosis on a substantial proportion of HF patients enables the physician to choose the best management strategy tailored to the patient's imaging findings. Moreover, CMR is ideally suited to monitor treatment and disease progression, because of high measurement accuracy/reproducibility and because patients can undergo serial CMR scans without exposure to ionizing radiation.

The identification of prognostic markers in patients with HF of either ischemic or nonischemic etiology is of paramount importance in the era of evidence-based cardiology. Sophisticated therapeutic options such as implantable cardioverter-defibrillators and biventricular pacemakers are now available, and the identification of patients who benefit most from these expensive therapies is becoming an increasing necessity.

CMR and Specific Causes of HF

The CMR techniques described above, and particularly the development of LGE-CMR, have revolutionized the role of CMR in the evaluation of HF patients. Currently, a comprehensive CMR protocol including anatomy, function, and LGE imaging is able to identify the underlying etiology in a substantial proportion of HF patients.

Ischemic cardiomyopathy. VIABILITY. Ischemic cardiomyopathy is characterized by areas of scarring that typically involve the subendocardium, and depending on the size of the infarct, extend up to the epicardium in a pattern consistent with the "wave front phenomenon" of ischemic cell death (25). With the development and extensive histopathological validation of the LGE technique, CMR has

JACC Vol. 54, No. 15, 2009
October 6, 2009:1407–24

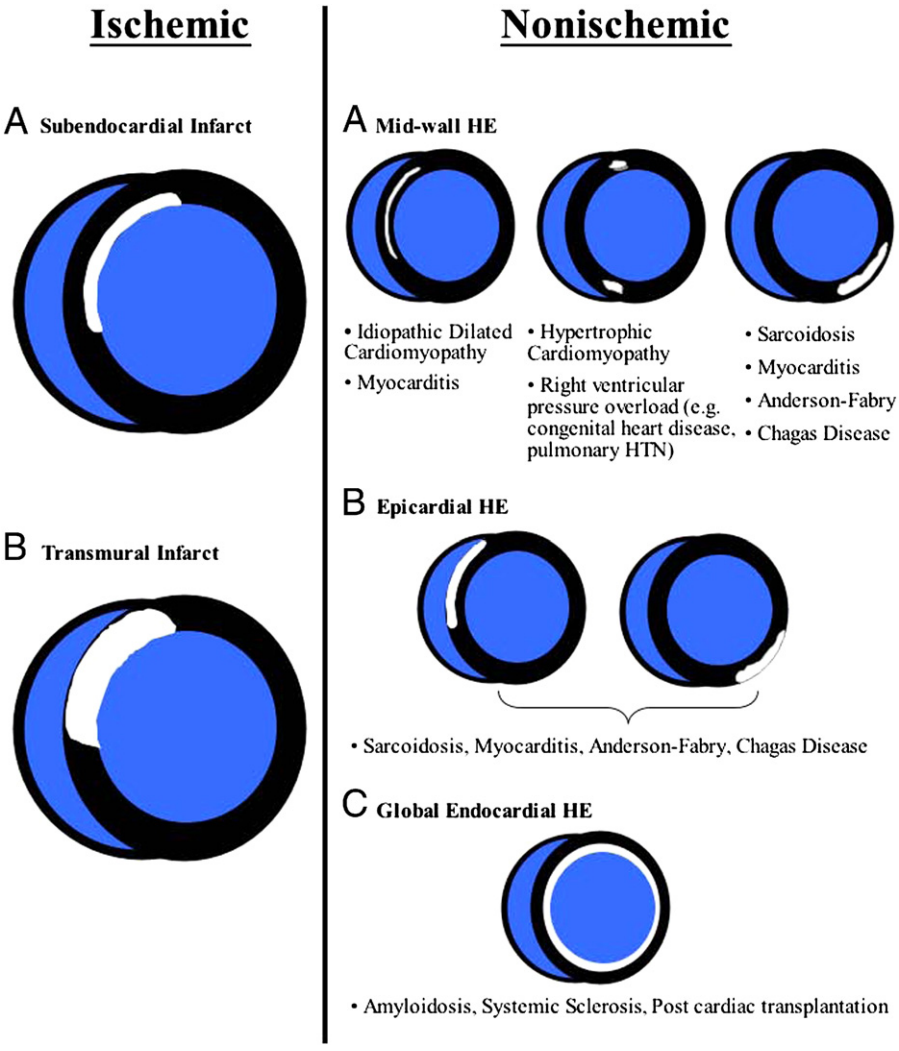

Figure 1 **HE Patterns for Ischemic and Nonischemic Disorders**

A schematic representation of hyperenhancement (HE) patterns that are characteristic for ischemic and nonischemic disorders. Note that the area of HE in ischemic cardiomyopathy always involves the subendocardium. In contrast, midwall or epicardial HE strongly suggests a nonischemic etiology. Reprinted, with permission, from Shah et al. (19). HTN = hypertension.

become the noninvasive gold standard modality for visualizing irreversibly injured myocardium (Fig. 2) and assess its transmural extent (26,27). The superb spatial resolution of LGE-CMR allows the detection of even small subendocardial infarcts that might otherwise be missed by lower spatial resolution techniques such as single-photon emission computed tomography (28). The ability of LGE-CMR to predict segmental functional recovery post-revascularization was a major breakthrough. In a seminal paper, Kim et al. (29) showed an inverse relationship between the transmural extent of myocardial infarction and recovery of segmental contractile function after revascularization. Multiple studies have confirmed the ability of LGE-CMR to predict recovery of contractile function post-revascularization in both the acute and the chronic infarct setting (30,31). Although some uncertainty exists regarding the predictive value of LGE-CMR in segments with an intermediate (25% to 75%) transmural extent of scarring, overall, LGE-CMR has the major advantage of assessing viability without the need to stress the patient, and thus has become the routine CMR procedure for this indication (32). A low-dose dobutamine study may be helpful in equivocal cases, but in practice this is rarely needed (33,34).

LGE-CMR not only defines the location and extent of infarction, but also differentiates areas that show failure of tissue perfusion after revascularization, the so-called no-reflow phenomenon. Extensive microcirculatory damage, myocyte necrosis, and localized edema that compresses intramural vessels result in delayed penetration of the contrast to the core of the infarction. This generates a

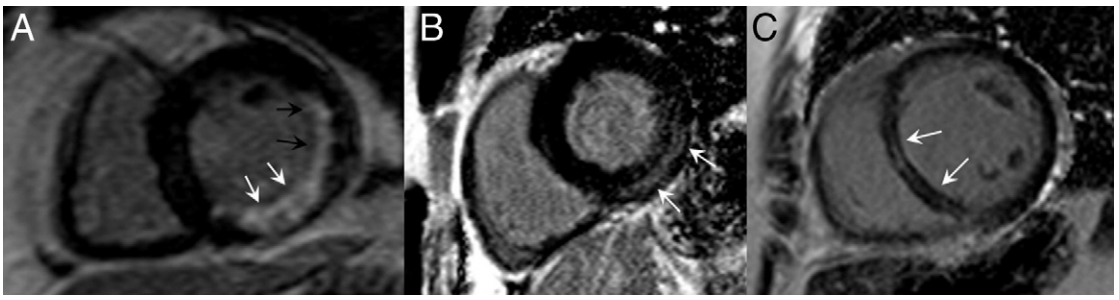

Figure 2 **Three Characteristic Examples of Late Gadolinium Enhancement**

(A) Ischemic cardiomyopathy: previous myocardial infarct with transmural extent of scarring **(white arrows)** in the inferior wall, but only subendocardial (<50%) scar in the inferolateral region **(black arrows)**. **(B)** Myocarditis: midwall late enhancement in the inferolateral wall **(white arrows)**. **(C)** Dilated cardiomyopathy: midwall late gadolinium enhancement in the septum **(white arrows)**.

central black area within a larger surrounding region of hyperenhancement (Fig. 3). Such microvascular obstruction detected by CMR has been linked to aggravated ventricular remodeling and adverse cardiovascular events after acute myocardial infarction (35,36).

REVERSIBLE VERSUS IRREVERSIBLE INJURY. The combination of LGE and T2-weighted imaging enables CMR to differentiate between acute and chronic injury. In acute myocardial infarction, T2-weighted images can detect an area of high signal caused by tissue edema that exceeds that of irreversible injury (37) and represents the area at risk. Furthermore, edema imaging detects acute ischemic myocyte injury before the onset of irreversible myocyte injury (38). This type of imaging is particularly appealing because it allows the detection of the extent of the ischemic zone even when the coronary artery is reperfused (39). Thus, CMR has an unprecedented capability to visualize the amount of salvaged myocardium, and this can be achieved retrospectively as late as 3 days after the insult. This method heralds a new era of clinical trials on salvage strategies in primary percutaneous coronary intervention. In clinical practice, T2-weighted imaging improves the overall accuracy of CMR in identifying patients with acute coronary syndromes (40). Edema imaging is an application that still needs further validation and refinement, however, to optimize both acquisition and quantitative analysis. Traditional edema-sensitive CMR methods using turbo spin-echo sequences are limited by artifacts leading to false-negative (e.g., posterior wall signal loss caused by through-plane motion) or false-positive results (bright rim artifacts caused by stagnant blood along the endocardial surface) (41). To overcome these problems, bright blood T2-weighted methods have been developed that increase the diagnostic accuracy and improve the reliability of CMR edema imaging (41,42).

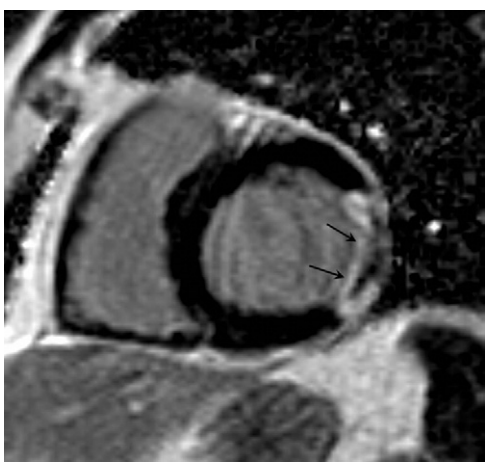

Figure 3 **Microvascular Obstruction on Late Gadolinium Enhancement Imaging**

A patient with recent myocardial infarction and evidence of microvascular obstruction on late gadolinium enhancement imaging. Note the hypoenhanced **(black)** area in the lateral wall **(black arrows)** completely surrounded by hyperenhanced regions.

OTHER SEQUELAE OF MYOCARDIAL INFARCTION. Complications of myocardial infarction, such as LV mural thrombus and aneurysmal dilation, can readily be recognized with CMR (43,44). Although small thrombi may be visible on cine images, confirmation on early post-contrast images is recommended. Thrombi are avascular structures, and hence on inversion recovery images acquired post-contrast appear as low-signal-intensity masses surrounded by high-signal-intensity areas such as cavity blood and/or hyperenhanced myocardial scar (Fig. 4) (43). The 3-dimensional shape and dyskinesis of true and false aneurysms can be reliably detected by cine CMR. Other complications of infarction, such as papillary muscle involvement causing mitral regurgitation and rupture of the interventricular septum, can also be characterized by CMR.

STRESS-INDUCIBLE ISCHEMIA. Multiple studies have proven the clinical feasibility, safety, and high diagnostic

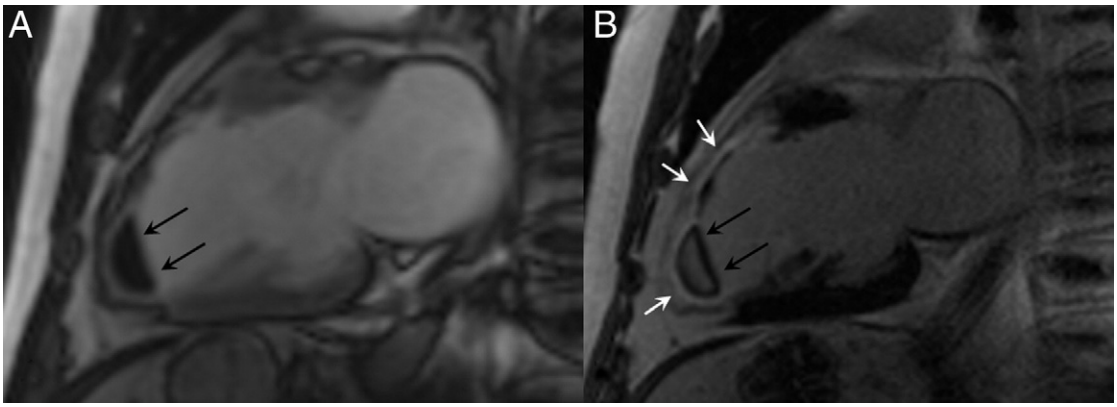

Figure 4 **Large Apical Thrombus in a Patient With Recent Transmural Anterior Infarct**

Images acquired early (1 to 3 min) **(A)** and late (>10 min) **(B)** after gadolinium administration showing a large intracavitary thrombus within the left ventricular apex **(black arrows)** in a patient with a large transmural anterior infarct **(white arrows)**.

accuracy of first-pass perfusion CMR with vasodilator stress for the detection of coronary artery disease (CAD) (45–50). A recent meta-analysis of 14 single-center studies (1,183 patients) showed a pooled sensitivity of 91% and specificity of 81% compared with conventional X-ray coronary angiography (45). A multicenter, multivendor trial recently showed that adenosine CMR perfusion is a valuable alternative to single-photon emission computed tomography for CAD detection showing at least equal diagnostic performance in a head-to-head comparison (51). Dobutamine stress CMR is an alternative technique for detecting CAD. Its safety and high diagnostic accuracy have been proven in several single-center studies (52,53). Patients with poor echo windows can be readily studied with a CMR dobutamine protocol (54).

CORONARY IMAGING. Imaging of the coronary arteries is not a standard clinical application of CMR. The small size and tortuous course of the coronary arteries, which move rapidly because of cardiac contraction and respiratory motion, make MR coronary angiography a demanding technique. Very high spatial and temporal resolution is required for this application, and although some progress has been made, reliable assessment of coronary stenoses by CMR is still challenging, with sensitivity and specificity showing a wide range: 50% to 94% and 50% to 100%, respectively (55). Consequently, the most recent clinical guidelines only support the use of CMR coronary angiography for the identification of anomalous coronary artery origins (55).

Dilated cardiomyopathy (DCM). The differentiation between ischemic and nonischemic causes of HF is a common challenge in clinical practice. The demonstration of normal coronary arteries on angiography is not sufficient on its own to exclude CAD as the underlying cause of HF. CMR, and in particular the LGE technique, is useful to determine whether LV dysfunction has an ischemic etiology. Up to 13% of patients diagnosed with DCM show areas of subendocardial or transmural LGE strongly suggestive of prior infarction (56,57). This may be caused by spontaneous recanalization after an occlusive coronary event, vasospasm, or embolization from minimally stenotic but unstable plaque. CMR has high sensitivity (81% to 100%) to detect underlying CAD in patients with poor LV function (56,58). In contrast, 10% to 26% of DCM patients without features of infarction show patchy or longitudinal striae of midwall hyperenhancement unrelated to a particular coronary artery territory (Fig. 2) (56,58). This distinct pattern of LGE corresponds to focal fibrosis at autopsy (59). It should be borne in mind that the total absence of LGE does not completely rule out ischemic cardiomyopathy in the rare setting of global myocardial hibernation. Multiple studies have now confirmed the use of CMR as a powerful tool for classifying patients with HF and LV systolic dysfunction with regard to the presence or absence of underlying CAD (57,58). Moreover, LGE-CMR can help to identify the arrhythmogenic substrate and plan an appropriate mapping and ablation strategy in patients with DCM (60).

Myocarditis. Acute myocarditis may present as new-onset HF, and its diagnosis is usually one of exclusion. The ultimate proof that the patient has myocarditis may be provided by endomyocardial biopsy, but the patchy nature of the disease increases the sampling error and limits its diagnostic role. Friedrich et al. (61) were the first to propose CMR for the noninvasive diagnosis of acute myocarditis. Using T1-weighted images, they found that the myocardium in patients with suspected myocarditis often has higher signal intensity relative to skeletal muscle (61). More recently, Abdel-Aty et al. (62) reported that a combined CMR approach using T2-weighted images and LGE provides high diagnostic accuracy for the identification of patients with acute myocarditis. The T2-weighted images early after symptom onset may show subepicardial and midwall areas of increased signal defining focal areas of myocardial edema. The LGE pattern in the setting of

myocarditis has a characteristic distribution (Fig. 2), and importantly, has been shown to have additional value in the detection of active myocarditis as defined by histopathology (63). The subepicardium is usually affected with varying degrees of progression toward the midmyocardial wall and typical sparing of the subendocardium, and the lateral and inferolateral walls are frequently involved (64). A different pattern of midwall septal LGE has been associated with human herpesvirus 6 or combined herpesvirus 6/Parvo B19 myocarditis (64). Although the presence of a typical LGE pattern is a strong indicator of the diagnosis, the absence of this pattern does not absolutely exclude myocarditis. The focal areas of hyperenhancement become diffuse over a period of days to weeks, then decrease during healing, and because of shrinking, may become invisible after recovery (63). Alternatively, large areas of scarring may still be visible after healing, causing distinctive linear midwall striae of hyperenhancement, a pattern similar to that seen in DCM patients (65). This finding suggests that previous myocarditis may be the underlying cause of LV dysfunction in a proportion of patients with DCM. Finally, CMR-guided endomyocardial biopsy may result in a higher yield of positive findings than routine RV biopsy (63).

Hypertrophic cardiomyopathy (HCM). HCM shows a wide variation of phenotypic expression. Asymmetric involvement of the interventricular septum is the most common form of the disease. Other variants include symmetric, apical, and mass-like LV hypertrophy. Some patients progress to an end-stage form, known as the burned-out phase, which is characterized by progressive wall thinning and systolic dysfunction. CMR has the ability to evaluate the heterogeneous appearances of HCM better than any other imaging modality (66–68). It can define the site of hypertrophy, allowing the visualization of areas difficult to assess with echocardiography, such as the posterolateral wall or the apex, and determine precisely the extent of hypertrophy (67–69). Moreover, echocardiography may underestimate the magnitude of LV hypertrophy (in one study reported as maximal wall thickness 24 ± 3 mm by echocardiography versus 32 ± 1 mm by CMR), which may be related to the difficulty of reliably imaging all segments (67). This is important clinically given that maximal wall thickness >30 mm is a major prognostic indicator in these patients (70). CMR is also useful in assessing papillary muscle abnormalities in HCM (anteroapical displacement or double bifid papillary muscles) that have been associated with LV outflow track obstruction independent of wall thickness (71).

Crucially, LGE-CMR identifies foci of diffuse scarring that may exist not only in severely hypertrophied myocardium but also (although less frequently) in regions with normal wall thickness (67). The pattern of LGE in HCM is patchy, typically midwall, and commonly involves the LV–RV junctions (Fig. 5) (72). It may also involve the apex in the apical variant of the disease (73). An exception to the patchy nature of LGE in HCM is in areas of burned-out myocardium, where the LV wall is typically thinned and enhancement may be full thickness. Although this resembles the pattern of LGE in patients with chronic transmural myocardial infarction, in burned-out HCM the areas of fibrosis typically do not conform to a particular coronary artery territory (74). Histopathological CMR correlation studies strongly relate the presence of hyperenhancement in HCM to areas of increased collagen deposition (75). Clinical studies have reported CMR-detected rates of fibrosis in up to 80% of HCM patients studied, with the variation across studies probably accounted for by the widely variable patient populations studied (76,77) and the limitations of detection in very diffuse fibrosis. The incidence of myocardial fibrosis increases with increasing wall thickness, and vasodilator reserve is reduced, particularly in the endocardium, and in proportion to the magnitude of hypertrophy (78). Finally, an important underappreciated feature of HCM, the presence of LV apical aneurysms, has been recently identified by CMR and linked with a high rate of adverse events (79).

Arrhythmogenic right ventricular cardiomyopathy (ARVC). ARVC is an inherited disease characterized by enlargement, dysfunction, and fibrofatty replacement of the RV (80). Biventricular disease variants have also been recognized, and in some cases, the LV may be the predominantly affected chamber (81,82). ARVC has a broad clinical spectrum and may present with ventricular tachyarrhythmias, sudden death, or HF. Its diagnosis is based on a set of major and minor criteria and generally requires an integrated assessment of electrical, functional, and anatomic abnormalities. Echocardiography and CMR are the most commonly used imaging modalities in the diagnostic workup of this entity. Compared with echocardiography, CMR can better visualize the RV in multiple planes (axial, sagittal, short-axis, and RV long-axis orientation) and detect both functional and structural features of ARVC. Functional abnormalities include regional wall motion defects, focal aneurysms, global RV dilation, and dysfunction (Fig. 6, Online Video 1) (83). The morphological abnormalities include focal wall thinning, wall hypertrophy, trabecular hypertrophy and disarray, moderator band hypertrophy, RV outflow tract enlargement, and intramyocardial fatty infiltration (84). Of these, localized aneurysms, severe global/segmental RV dilatation, and global systolic dysfunction are considered major criteria, whereas mild global/segmental dilatation of the RV, regional contraction abnormalities, and global diastolic dysfunction are considered minor criteria according to the task force (85). Recent studies have highlighted the role of CMR in detecting fibrosis of the RV myocardium in patients with ARVC (86,87). The presence of LGE correlates well with fibrofatty replacement on endomyocardial biopsy and predicts inducible ventricular tachycardia during electrophysiological studies, which may have important implications for risk stratification (86). The detection of fibrofatty replacement is difficult, however, because of its

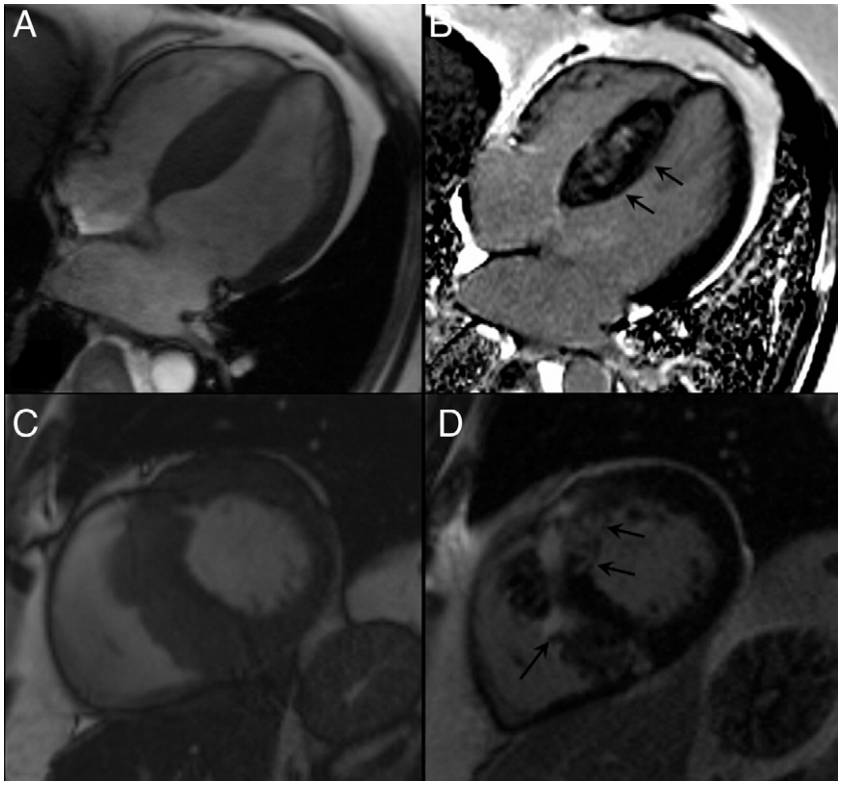

Figure 5 **Example of a Patient With Hypertrophic Cardiomyopathy**

(A) Still frame from horizontal long-axis cine sequence showing marked septal hypertrophy. **(B)** Same view with late gadolinium enhancement imaging showing patchy areas of scarring in the hypertrophied septum **(black arrows)**. **(C)** Still frame from a short-axis cine sequence of the same patient illustrating the asymmetric septal hypertrophy. **(D)** Same short-axis view with late gadolinium enhancement imaging showing the marked diffuse fibrosis within the thickened septum involving both left and right ventricular junctions **(black arrows)**.

diffuse nature, mixing with normal myocardial tissue and the thin RV wall combined with partial volume effects. The identification of fatty infiltration in the RV wall using T1-weighted images (with and without fat suppression) is not a Task Force criterion, has poor sensitivity and specificity, and is in fact the least reproducible CMR parameter (88). In contrast, the detection of global and regional RV wall motion abnormalities is highly specific to the disease (88). However, experience is needed and caution should be exercised in interpreting results, especially in the absence of wall motion abnormalities. It should also be borne in mind that regions close to the moderator band may show contraction abnormalities, which in isolation do not represent findings positive for ARVC. Despite the controversies surrounding its role in ARVC, CMR is a valuable diagnostic tool that substantially improves the sensitivity of clinical diagnosis, particularly in early or incompletely expressed disease (89).

Iron overload cardiomyopathy. Heart failure caused by iron overload is the leading cause of death in patients with beta-thalassemia major (90). Cardiac siderosis can also be found in other transfusion-dependent anemias and in primary hemochromatosis. The cardiomyopathy is reversible if chelation is commenced early, but diagnosis is often delayed because of the late onset of symptoms. Myocardial iron overload can be quantitatively assessed by T2* CMR imaging, with profound implications for the clinical management of these patients (91,92). T2* is a parameter related to but distinct from T2 that decreases when regional magnetic field homogeneity is reduced in the vicinity of iron. In contrast, there is no significant correlation between myocardial T2* and the conventional parameters of iron status, such as serum ferritin or liver iron load (91). As myocardial iron increases, there is a progressive decline in ejection fraction and all patients with HF have a myocardial T2* of $<$20 ms. This is useful to guide treatment and monitor response to iron-chelating drug regimens (93,94).

Amyloidosis. Cardiac involvement in systemic amyloidosis is frequent. The heart in AL amyloidosis (the most common form) is affected in up to 50% of cases, and congestive HF is the presenting clinical manifestation in about one-half of these patients (95). Once congestive HF occurs, the median survival is $<$6 months in untreated patients; therefore, early recognition of the disease and prompt initiation of therapy is critical. Characteristic structural and functional features of cardiac amyloidosis can be detected by CMR imaging, such

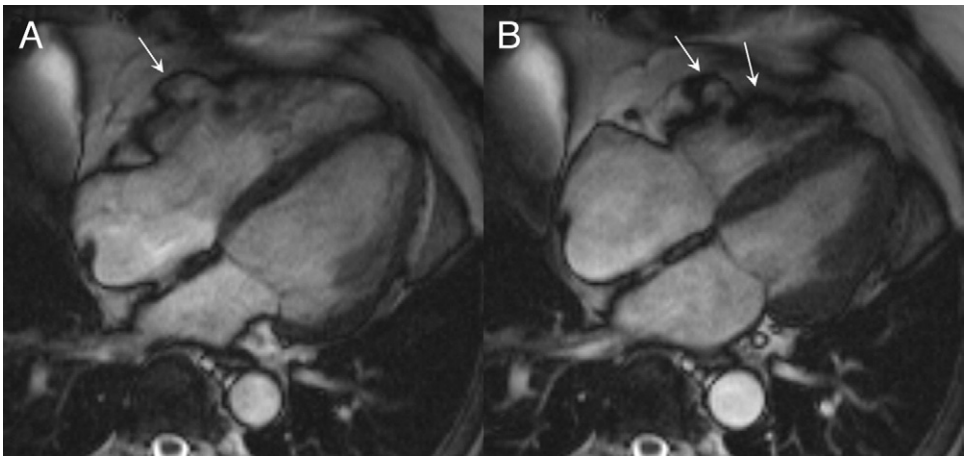

Figure 6 **Example of a Patient With Arrhythmogenic Right Ventricular Cardiomyopathy**

Still frames from a horizontal long-axis cine sequence in end diastole **(A)** and end systole **(B)** showing prominent aneurysmal areas in the right ventricular free wall **(white arrows)**. See also Online Video 1.

as concentric hypertrophy with normal or reduced contractility, thickened interatrial septum, and bi-atrial dilation (95). After gadolinium administration, there may be a circumferential pattern of LGE, preferentially affecting the subendocardium but sometimes showing a more patchy transmural pattern (Fig. 7) (95–97). The wash-in and washout kinetics of gadolinium are markedly abnormal when amyloid fibrils are accumulated in the myocardial interstitium, which results in unique LGE appearances. There may be a characteristic zebra-stripe appearance with subendocardial enhancement of the LV and RV endocardium, sparing the midwall of the interventricular septum. The blood pool appears atypically dark, reflecting high myocardial contrast uptake and fast blood pool washout. The LGE-CMR and cardiac biopsy findings were correlated in a study of 33 patients presenting with diastolic HF in combination with either myocardial hypertrophy and/or other conditions often associated with cardiac amyloidosis (98). A typical pattern of circumferential subendocardial LGE was observed in 12 of 15 patients (sensitivity 80%) with subsequent biopsy-proven cardiac amyloidosis, compared with only 1 individual in the group of 18 patients (specificity 94%) diagnosed with other myocardial diseases. Although cardiac involvement is considered a late manifestation of systemic amyloidosis, in 11 of 15 patients with positive biopsy, cardiac involvement was the first manifestation of disease (98). This may in part reflect the ability of LGE-CMR to detect early cardiac involvement when morphological changes are not apparent by echocardiography or nuclear techniques.

Sarcoidosis. Myocardial involvement occurs in at least 25% of patients with sarcoidosis at autopsy. However, fewer than one-half of them have signs or symptoms of cardiac involvement (99,100), making antemortem diagnosis of cardiac sarcoidosis an exceptional challenge. Progressive congestive HF has been shown to be the cause of death in 25% of patients with cardiac sarcoidosis, making it the second most frequent cause of death after sudden death caused by arrhythmias (101,102). Thus, it is important to identify the presence of cardiac involvement in these patients who may benefit from medical and/or implantable defibrillator therapy. Cardiovascular MR can show some of the characteristic features of cardiac sarcoid (e.g., septal thinning, LV/RV dilation and systolic dysfunction, or pericardial effusion) (Fig. 8) (101,103). Moreover, several studies have shown the usefulness of LGE-CMR in the detection of cardiac sarcoidosis and evaluation of response to steroid treatment (104,105). The LGE in these patients usually shows a nonischemic pattern with hyperenhancement of the midmyocardial wall or the epicardium in an unpredictable distribution (7). However, subendocardial or transmural hyperenhancement has also been observed, mimicking an ischemic pattern. The anteroseptal and inferolateral walls are most frequently involved, although sometimes hyperenhancement is seen in other territories, including the RV (106). Follow-up studies showed that the enhanced areas were notably diminished in size and intensity after steroid treatment (107). The LGE-CMR scan can also be used to guide endomyocardial biopsy in sarcoidosis. Additionally, T2-weighted sequences may monitor disease activity by the identification of edematous areas associated with inflammation and granulomatous lesions (108).

Anderson-Fabry disease. Anderson-Fabry disease is an X-linked disorder of lysosomal metabolism caused by the partial or complete deficiency of the enzyme alpha-galactosidase A, which results in the accumulation of excess cellular glycosphingolipid within the blood vessels and heart (109). This is a cause of LV hypertrophy associated with progressive myocardial fibrosis and death from HF. CMR can be used to assess LV function, determine the pattern

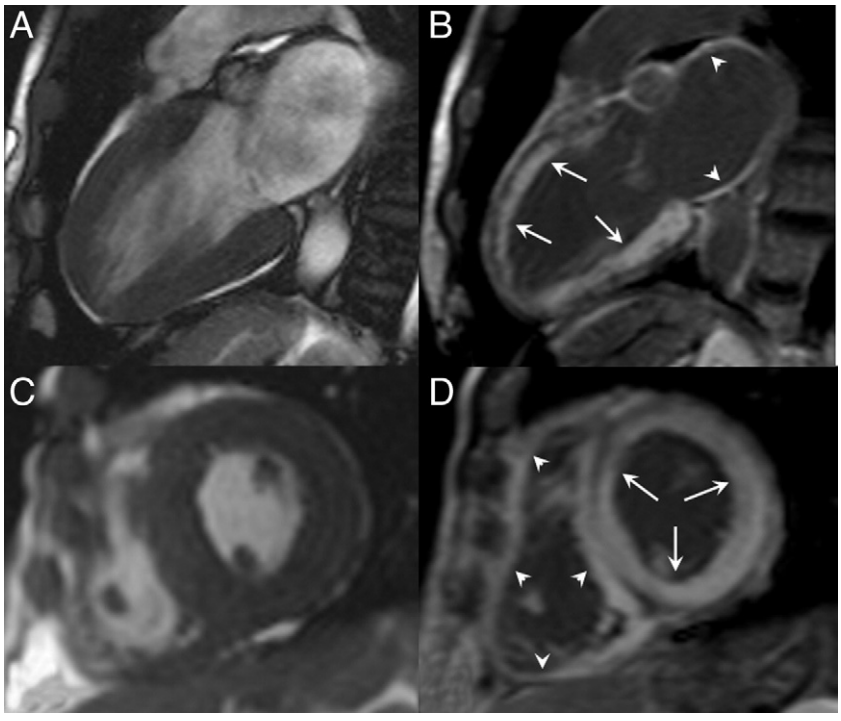

Figure 7 **Example of a Patient With Cardiac Amyloidosis**

Still diastolic frames from cines: vertical long- **(A)** and short-axis at the midventricular level **(C)** showing moderate concentric hypertrophy. **(B and D)** Corresponding images using the late gadolinium enhancement technique, respectively. The vertical long-axis image **(B)** shows diffuse, predominantly subendocardial enhancement in the left ventricle **(white arrows)** and atrium **(white arrowheads)**. The short-axis image **(D)** shows a ring of subendocardial hyperenhancement in the left ventricle **(white arrows)**. The septum shows biventricular subendocardial enhancement with a dark midwall (zebra appearance). There is also widespread hyperenhancement in the right ventricle **(white arrowheads)**. Note the dark blood pool.

and extent of LV hypertrophy, and identify areas of fibrosis. The LGE pattern typically spares the subendocardium and shows a striking predilection for the basal inferolateral LV segments. Histological data suggest that these areas of LGE correspond to regions of replacement fibrosis (110). Up to 6% of patients who are initially diagnosed with HCM actually have evidence of Anderson-Fabry disease (111). The implications of an incorrect diagnosis are considerable

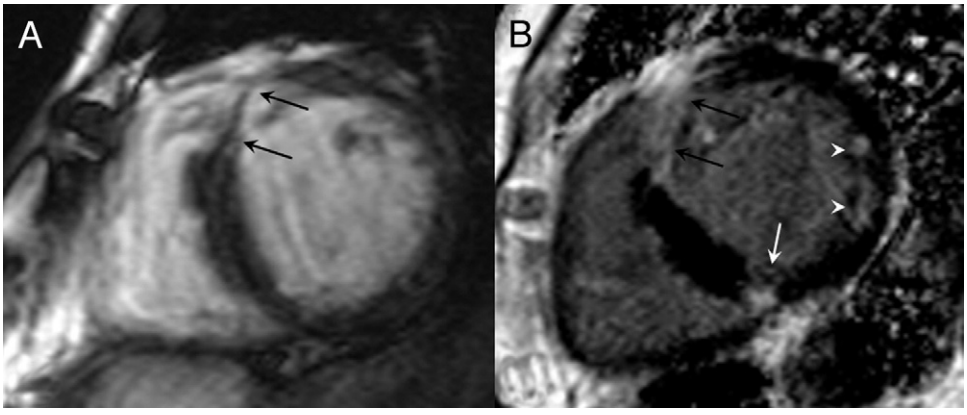

Figure 8 **Example of a Patient With Sarcoidosis**

(A) Still frame from short-axis cine sequence showing an area of marked thinning in the anterior septum. **(B)** Same view after gadolinium administration showing 3 different patterns of fibrosis. Transmural hyperenhancement corresponding to the area of septal thinning **(black arrows)**, subepicardial hyperenhancement in the inferior right ventricular insertion point **(white arrow)**, and midwall enhancement in the inferolateral wall **(white arrowheads)**.

because patients with Anderson-Fabry disease respond to enzyme replacement therapy, including an improvement in cardiac function and regression of hypertrophy (112,113). Ideally, the administration of recombinant alpha-galactosidase A should be started before myocardial fibrosis has developed to achieve long-term improvement in myocardial morphology, function, and exercise capacity (114). Anderson-Fabry disease should always be considered if unexplained LV hypertrophy is seen, particularly in a young patient.

Constrictive pericarditis. The normal pericardium appears as a hypointense line usually less than 2 mm thick, and indeed sometimes not visible on CMR images. CMR can diagnose constrictive pericarditis by providing morphological evidence of an abnormally thickened pericardium associated with constrictive physiology (115). On black blood anatomical CMR images, a pericardial thickness of more than 4 mm is suggestive of constriction (Fig. 9). In addition, free-breathing real-time cine CMR can depict 2 important features: increased ventricular coupling with early inspiratory flattening of the interventricular septum in diastole and dilation of the inferior vena cava, which shows little change in size during respiration. These findings may help differentiate constrictive pericarditis from restrictive cardiomyopathy (116). Finally, the use of tagged cine imaging can aid in identifying nonadherence of the visceral and parietal pericardium throughout the cardiac cycle.

LV noncompaction. LV noncompaction is characterized by prominent LV trabeculations with deep intertrabecular recesses, resulting in a distinct noncompacted layer lining the LV cavity. Echocardiography without contrast may misdiagnose LV noncompaction as apical HCM (117). CMR can reliably discriminate among apical HCM, mild-normal trabeculations, and grossly trabeculated LV myocardium with intertrabecular recesses. A ratio of noncompacted to compacted myocardium >2.3 yields high sensitivity (85%) and specificity (99%) in the diagnosis of this condition (118).

Chagas disease. Chagas disease is caused by *Trypanosoma cruzi* infection. Cardiac involvement is the most serious long-term complication, occurring in approximately one-third of seropositive individuals, and is a major cause of death from HF in Latin America. It is characterized by progressive myocardial fibrosis, which can be identified with LGE-CMR in many patients, not only with advanced disease but also in seropositive subjects without clinical symptoms or wall motion abnormalities (119). The LV apex and inferolateral regions are the sites where fibrosis is most commonly seen. There is an overlap of reported LGE patterns with both ischemic (subendocardial or transmural) and nonischemic patterns (subepicardial, midwall) (119). Additionally, CMR can detect the consequences of progressive myocardial damage in Chagas disease such as localized areas of thinning with hypokinesis or akinesis and aneurysm formation, with global ventricular dysfunction (120).

Other cardiomyopathies. Other less common myocardial diseases that result in HF can be identified by CMR. Churg-Strauss syndrome is a rare form of small-vessel vasculitis that can lead to symptomatic HF with poor prognosis. In 11 patients with Churg-Strauss syndrome confirmed by biopsy, a subendocardial pattern of fibrosis in the absence of CAD was found (121). Moreover, CMR allows the detection of endomyocardial fibrosis, providing a comprehensive tool for the early diagnosis of this rare but severe disease. The exclusive involvement of endomyocardium on LGE-CMR in conjunction with normal myocardial function, apical obliteration, and thrombus formation are typical findings in these patients (122). Stress (Tako-Tsubo) cardiomyopathy is another entity that can be readily identified and characterized by CMR. Affected patients typically do not show areas of scarring on LGE despite

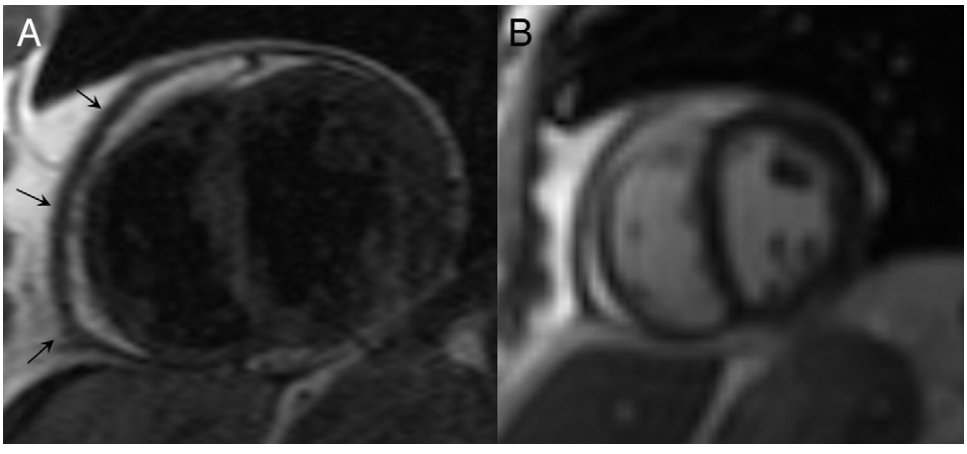

Figure 9 Example of a Patient With Pericardial Constriction

(A) T1-weighted spin-echo image showing an area of markedly thickened pericardium (measuring up to 6 mm, **black arrow**) overlaying the right ventricular free wall. **(B)** Real-time free-breathing cine revealed the presence of early inspiratory flattening of the interventricular septum in diastole resulting in a D-shaped left ventricle.

characteristic wall motion defects mimicking anteroapical infarction (123,124), but may have evidence of edema on T2-weighted images (125).

Cardiac masses. Cardiac masses can occasionally manifest as new-onset HF (126). CMR imaging with tissue characterization techniques—T2-weighted, T1-weighted, first-pass perfusion, and LGE—is an ideal method for their assessment (Fig. 10, Online Video 2). It provides precise anatomical, functional, and morphological information, including differentiation from thrombus, often allowing the specific diagnosis of the mass (127). Furthermore, CMR has the ability to differentiate intracardiac masses from masses that externally compress the heart and also to show invasion of surrounding structures.

Valvular heart disease. CMR provides information on valve anatomy (although echocardiography is better for assessing valve structure) and allows excellent quantitative evaluation of stenosis and regurgitation (18). Importantly, CMR can also assess accurately the consequences of the valvular lesion on the myocardium, including the effects on ventricular volumes and mass and alterations in systolic function. The high reproducibility of CMR-derived ventricular volumes enables the detection of modest changes with serial scanning, and can potentially allow earlier identification of LV parameters indicating a detrimental course. CMR-derived measures of valve dysfunction (such as regurgitant volume and fraction) may in the future become important for planning the correct timing of valve replacement.

Congenital heart disease. CMR provides a wealth of anatomical and physiological information in patients with congenital cardiac abnormalities (128), which are a more rare cause of HF. The detailed description of the use of CMR in such patients is beyond the scope of this article.

Assessment of Mechanical Dyssynchrony With CMR

Echocardiography has played a major role in the assessment of mechanical dyssynchrony and the selection of patients for cardiac resynchronization therapy (CRT). However, despite the use of sophisticated tools such as tissue Doppler methods to predict response to CRT, approximately 20% to 30% of patients do not show clinical improvement (129,130). CMR is emerging as an alternative technique for selecting CRT candidates with an increased probability of responding. Mechanical dyssynchrony can be assessed using various CMR techniques, such as cine wall motion, myocardial tagging, tissue velocity mapping, or displacement imaging (131,132). Recent studies have suggested that a large scar burden, a history of ischemic HF or myocardial infarction, and fewer viable myocardial segments are associated with nonresponse to CRT (133–136). In addition to total scar burden, it has been shown that the location of scar tissue within the myocardium may play an important role for the response to CRT, and the presence of scar in the septal (133) or posterolateral wall (136) significantly decreases the response rate to CRT. Finally, CMR can be used to assess coronary venous morphology before CRT, which may help to determine whether the area with the greatest electrical and mechanical activation delay can be reached through the venous anatomy or whether epicardial lead placement would be more appropriate (137).

CMR for Cardiac Stem Cell Therapy

Stem cell therapy aiming to repair irreversibly injured myocardium is being intensively studied. CMR imaging seems uniquely suited to become an integral part of this

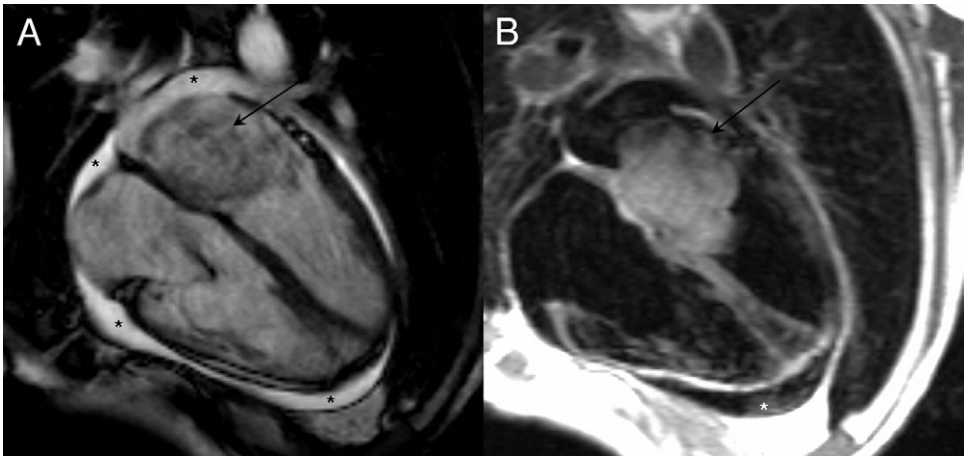

Figure 10 Example of a Patient With a Large Atrial Myxoma

(A) Still frame from horizontal long-axis cine sequence showing the tumor almost filling the entire left atrium **(black arrow)**. **(B)** T1-weighted turbo spin-echo image on the same view with the mass **(black arrow)** appearing to prolapse through the mitral valve obstructing flow to the ventricle, therefore resulting in functional mitral stenosis. The patient presented with dyspnea and had increased systolic pulmonary pressure (60 mm Hg) on echocardiography. Note also the circumferential pericardial effusion **(*)**. See also Online Video 2.

therapy by providing a platform to assess functional parameters such as LV function and size, myocardial perfusion, infarct size, and myocardial viability (138). Moreover, CMR can be used for in vivo tracking of stem cells to evaluate both their short-term distribution and their long-term survival (138,139). Although CMR has high spatial resolution, its sensitivity with reference to the detectable levels of tracers (10^{-5} mol/l) is relatively low compared with radioisotope-labeled (10^{-11} to 10^{-12} mol/l) and optical (10^{-15} to 10^{-17} mol/l) imaging (139). Imaging at higher field strengths (3.0-T or higher) and the use of better labeling agents may improve the sensitivity of CMR to detect therapeutic cell delivery.

Prognostic Information From CMR in HF

Although CMR, and particularly the LGE or first-pass perfusion techniques, are relatively new imaging tools, data on the prognostic role of CMR imaging in patients with HF are rapidly becoming available.

Ischemic cardiomyopathy. Infarct size determined by LGE-CMR is a better predictor of inducible ventricular tachycardia on electrophysiological studies than LV ejection fraction (140). In addition, the extent of the peri-infarct zone assessed by CMR has been related to all-cause mortality (141). Increased infarct tissue heterogeneity identified by CMR augments the susceptibility to ventricular arrhythmias in patients with prior myocardial infarction and LV dysfunction (142). Quantification of RV ejection fraction by CMR late after myocardial infarction is an important predictor of prognosis adjusted for patient age, LV infarct size, and LV ejection fraction (143). Microvascular obstruction detected by CMR predicts aggravated ventricular remodeling and adverse cardiovascular events after acute myocardial infarction (35). Among patients with a clinical suspicion of CAD but without a history of myocardial infarction, the identification of LGE involving even a small amount of myocardium (mean LV mass 1.4%) carries a high risk of future cardiac events with incremental prognostic value beyond common clinical, angiographic, and functional predictors (144). Finally, in patients with known or suspected CAD, myocardial ischemia detected by adenosine, dipyridamole, or dobutamine stress CMR can be used to identify individuals at high risk for subsequent cardiac death, nonfatal myocardial infarction, or congestive HF (145–147).

DCM. In DCM patients with symptomatic HF, a pattern of midwall fibrosis was associated with a high rate of all-cause mortality and hospitalization even after adjustment for age, LV function, and ventricular volumes measured by CMR (148). Furthermore, adverse cardiac prognosis in DCM is associated with the presence of LGE regardless of segmental pattern (149). Patients who had LGE of any pattern showed an 8-fold higher risk of reaching a composite outcome of HF hospitalization, appropriate implantable defibrillator discharges, and cardiac death compared with patients without LGE. Similar to findings in ischemic cardiomyopathy, the presence of scarring on LGE-CMR in DCM is predictive of inducible ventricular tachycardia even after adjustment for LV ejection fraction (150).

HCM. A preliminary study in highly selected HCM patients older than 40 years of age showed an association between the presence of fibrosis on LGE-CMR and the likelihood of developing HF (76). More recently, it was shown that the presence of LGE was independently associated with ventricular tachyarrhythmias on an ambulatory electrocardiogram in a largely asymptomatic or mildly symptomatic cohort of HCM patients (151,152). LGE was associated with a 7-fold increase in the risk of nonsustained ventricular tachycardia and was the only independent predictor of this arrhythmia. Further prospective studies in large patient populations are required to establish the role of LGE as an independent predictor for sudden death or HF in HCM.

Amyloidosis. Recent evidence suggests that LGE carries unique prognostic information in amyloidosis. In 29 patients with proven cardiac amyloidosis, LGE was associated with significant survival differences (153). Moreover, the presence of LGE in patients with systemic amyloidosis is strongly associated with HF severity as assessed by B-type natriuretic peptide (154). Further confirmation from prospective studies on larger cardiac amyloidosis cohorts is needed. The long-term prognostic implications of LGE in cardiac sarcoidosis and myocarditis have yet to be determined.

Thalassemia. Recent evidence suggests that thalassemia major patients with heavy myocardial iron overload (myocardial T2* <10 ms) have a high risk of developing HF (155).

Future Perspective

It is anticipated that the application of CMR in the evaluation of patients with HF will expand substantially in the coming years. We predict that most patients with HF will eventually undergo CMR imaging as part of the diagnostic workup and to guide management and stratify risk. The list of proposed indications for the use of CMR in HF patients (Table 1) is likely to further expand in the near future (156). Improvement in software and hardware will further shorten scan times and allow the use of real-time imaging with better spatial and temporal resolution. New CMR techniques aiming at the identification and quantification of diffuse fibrosis will further improve the in vivo assessment of myocardial pathology (157). Novel CMR contrast agents will target specific tissue types for diagnosis and treatment. Stem cell therapy will be precisely monitored by CMR and retention of such cells by the heart will be documented. Interventional CMR will be increasingly used to guide therapeutic procedures such as closure of septal defects or the percutaneous placement of heart valves (158–160). Finally, MR spectroscopy (a method currently limited by its low spatial and temporal resolution) should allow reliable assessment of metabolic changes in the failing

Table 1 Proposed Indications for CMR Imaging in Patients With Heart Failure

Serial assessment of biventricular structure, size, and function (anatomy, LV/RV volumes, global and regional systolic function, mass)
Evaluation of native and prosthetic cardiac valves (planimetry of stenotic disease, estimation of peak stenotic velocities and gradients, quantification of regurgitant disease)
Evaluation of cardiac masses, differentiation between tumor and thrombus
Evaluation of great vessels and pulmonary veins
Determination of the location and extent of acute (including no-reflow regions) and chronic myocardial necrosis
Viability assessment before revascularization (LGE or low-dose dobutamine)
Determination of the area at risk in patients with acute myocardial infarction and the salvageable area post-revascularization with percutaneous coronary intervention
Identification of the presence and quantification of the extent of inducible ischemia (vasodilator perfusion or high-dose dobutamine stress CMR)
Evaluation of suspected anomalous coronary origins (MR coronary angiography)
Differentiation of ischemic versus nonischemic cardiomyopathy
Evaluation of myocarditis
Evaluation of specific cardiomyopathies (in vivo tissue characterization)
Dilated cardiomyopathy
Hypertrophic cardiomyopathy
Arrhythmogenic right ventricular cardiomyopathy
Cardiac amyloidosis
Cardiac sarcoidosis
Anderson-Fabry disease
Iron overload cardiomyopathy
Left ventricular noncompaction
Other less common diseases (e.g., Chagas disease, endomyocardial fibrosis, Churg-Strauss syndrome, and so on)
Assessment of mechanical dyssynchrony before resynchronization therapy
Patients with technically limited images from echocardiogram
Discordant information that is clinically significant from prior tests

Modified, with permission, from Hendel et al. (156).
CMR = cardiovascular magnetic resonance; LGE = late gadolinium; LV = left ventricular; MR = magnetic resonance; RV = right ventricular.

heart and monitoring of the response to novel forms of metabolic therapy (161).

Acknowledgment

The authors thank Dr. Matthew Robson, Oxford Centre for Clinical Magnetic Resonance Research (OCMR) Chief Cardiac Physicist, for feedback on the technical section.

Reprint requests and correspondence: Dr. Stefan Neubauer, Department of Cardiovascular Medicine, John Radcliffe Hospital, Headley Way, Headington, OX3 9DU Oxford, United Kingdom. E-mail: stefan.neubauer@cardiov.ox.ac.uk.

REFERENCES

1. Dayer M, Cowie MR. Heart failure: diagnosis and health care burden. Clin Med 2004;4:13–8.
2. Lloyd-Jones D, Adams R, Carnethon M, et al. Heart disease and stroke statistics—2009 update: a report from the American Heart Association Statistics Committee and Stroke Statistics Subcommittee. Circulation 2009;119:480–6.
3. Jessup M, Abraham WT, Casey DE, et al. Focused update: ACCF/AHA guidelines for the diagnosis and management of heart failure in adults. A report of the American College of Cardiology Foundation/American Heart Association Task Force on Practice Guidelines. J Am Coll Cardiol 2009;53:1343–82.
4. Abdel-Aty H, Simonetti O, Friedrich MG. T2-weighted cardiovascular magnetic resonance imaging. J Magn Reson Imaging 2007;26:452–9.
5. Schaefer S, Malloy CR, Katz J, et al. Gadolinium-DTPA-enhanced nuclear magnetic resonance imaging of reperfused myocardium: identification of the myocardial bed at risk. J Am Coll Cardiol 1988;12:1064–72.
6. Rehwald WG, Fieno DS, Chen EL, Kim RJ, Judd RM. Myocardial magnetic resonance imaging contrast agent concentrations after reversible and irreversible ischemic injury. Circulation 2002;105:224–9.
7. Mahrholdt H, Wagner A, Judd RM, Sechtem U, Kim RJ. Delayed enhancement cardiovascular magnetic resonance assessment of non-ischaemic cardiomyopathies. Eur Heart J 2005;26:1461–74.
8. Kim RJ, Chen EL, Lima JA, Judd RM. Myocardial Gd-DTPA kinetics determine MRI contrast enhancement and reflect the extent and severity of myocardial injury after acute reperfused infarction. Circulation 1996;94:3318–26.
9. Shellock FG, Crues JV. MR procedures: biologic effects, safety, and patient care. Radiology 2004;232:635–52.
10. Grobner T. Gadolinium—a specific trigger for the development of nephrogenic fibrosing dermopathy and nephrogenic systemic fibrosis? Nephrol Dial Transplant 2006;21:1104–8.
11. Grobner T, Prischl FC. Patient characteristics and risk factors for nephrogenic systemic fibrosis following gadolinium exposure. Semin Dial 2008;21:135–9.
12. Walsh TF, Hundley WG. Assessment of ventricular function with cardiovascular magnetic resonance. Cardiol Clin 2007;25:15–33, v.
13. Selvanayagam J, Westaby S, Channon K, et al. Images in cardiovascular medicine. Surgical left ventricular restoration: an extreme case. Circulation 2003;107:e71.
14. Karamitsos TD, Hudsmith LE, Selvanayagam JB, Neubauer S, Francis JM. Operator induced variability in left ventricular measurements with cardiovascular magnetic resonance is improved after training. J Cardiovasc Magn Reson 2007;9:777–83.
15. Mahrholdt H, Wagner A, Holly TA, et al. Reproducibility of chronic infarct size measurement by contrast-enhanced magnetic resonance imaging. Circulation 2002;106:2322–7.
16. Kilner PJ, Gatehouse PD, Firmin DN. Flow measurement by magnetic resonance: a unique asset worth optimising. J Cardiovasc Magn Reson 2007;9:723–8.
17. Sarwar A, Shapiro MD, Abbara S, Cury RC. Cardiac magnetic resonance imaging for the evaluation of ventricular function. Semin Roentgenol 2008;43:183–92.

18. Cawley PJ, Maki JH, Otto CM. Cardiovascular magnetic resonance imaging for valvular heart disease: technique and validation. Circulation 2009;119:468–78.
19. Shah DJ, Judd RM, Kim RJ. Myocardial viability. In: Edelman RR, Hesselink JR, Zlatkin MB, Crues JV, editors. Clinical Magnetic Resonance Imaging. 3rd edition. New York, NY: Elsevier, 2006.
20. Wang J, Nagueh SF. Current perspectives on cardiac function in patients with diastolic heart failure. Circulation 2009;119:1146–57.
21. Rathi VK, Doyle M, Yamrozik J, et al. Routine evaluation of left ventricular diastolic function by cardiovascular magnetic resonance: a practical approach. J Cardiovasc Magn Reson 2008;10:36.
22. Paelinck BP, Lamb HJ, Bax JJ, Van der Wall EE, de Roos A. Assessment of diastolic function by cardiovascular magnetic resonance. Am Heart J 2002;144:198–205.
23. Reichek N. MRI myocardial tagging. J Magn Reson Imaging 1999;10:609–16.
24. Oh JK, Hatle L, Tajik AJ, Little WC. Diastolic heart failure can be diagnosed by comprehensive two-dimensional and Doppler echocardiography. J Am Coll Cardiol 2006;47:500–6.
25. Reimer KA, Lowe JE, Rasmussen MM, Jennings RB. The wavefront phenomenon of ischemic cell death. 1. Myocardial infarct size vs duration of coronary occlusion in dogs. Circulation 1977;56:786–94.
26. Kim RJ, Fieno DS, Parrish TB, et al. Relationship of MRI delayed contrast enhancement to irreversible injury, infarct age, and contractile function. Circulation 1999;100:1992–2002.
27. Wagner A, Mahrholdt H, Thomson L, et al. Effects of time, dose, and inversion time for acute myocardial infarct size measurements based on magnetic resonance imaging-delayed contrast enhancement. J Am Coll Cardiol 2006;47:2027–33.
28. Wagner A, Mahrholdt H, Holly TA, et al. Contrast-enhanced MRI and routine single photon emission computed tomography (SPECT) perfusion imaging for detection of subendocardial myocardial infarcts: an imaging study. Lancet 2003;361:374–9.
29. Kim RJ, Wu E, Rafael A, et al. The use of contrast-enhanced magnetic resonance imaging to identify reversible myocardial dysfunction. N Engl J Med 2000;343:1445–53.
30. Selvanayagam JB, Kardos A, Francis JM, et al. Value of delayed-enhancement cardiovascular magnetic resonance imaging in predicting myocardial viability after surgical revascularization. Circulation 2004;110:1535–41.
31. Beek AM, Kuhl HP, Bondarenko O, et al. Delayed contrast-enhanced magnetic resonance imaging for the prediction of regional functional improvement after acute myocardial infarction. J Am Coll Cardiol 2003;42:895–901.
32. Kim RJ, Manning WJ. Viability assessment by delayed enhancement cardiovascular magnetic resonance: will low-dose dobutamine dull the shine? Circulation 2004;109:2476–9.
33. Kaandorp TA, Bax JJ, Schuijf JD, et al. Head-to-head comparison between contrast-enhanced magnetic resonance imaging and dobutamine magnetic resonance imaging in men with ischemic cardiomyopathy. Am J Cardiol 2004;93:1461–4.
34. Wellnhofer E, Olariu A, Klein C, et al. Magnetic resonance low-dose dobutamine test is superior to SCAR quantification for the prediction of functional recovery. Circulation 2004;109:2172–4.
35. Wu KC, Zerhouni EA, Judd RM, et al. Prognostic significance of microvascular obstruction by magnetic resonance imaging in patients with acute myocardial infarction. Circulation 1998;97:765–72.
36. Nijveldt R, Beek AM, Hirsch A, et al. Functional recovery after acute myocardial infarction: comparison between angiography, electrocardiography, and cardiovascular magnetic resonance measures of microvascular injury. J Am Coll Cardiol 2008;52:181–9.
37. Aletras AH, Tilak GS, Natanzon A, et al. Retrospective determination of the area at risk for reperfused acute myocardial infarction with T2-weighted cardiac magnetic resonance imaging: histopathological and displacement encoding with stimulated echoes (DENSE) functional validations. Circulation 2006;113:1865–70.
38. Abdel-Aty H, Cocker M, Meek C, Tyberg JV, Friedrich MG. Edema as a very early marker for acute myocardial ischemia: a cardiovascular magnetic resonance study. J Am Coll Cardiol 2009; 53:1194–201.
39. Friedrich MG, Abdel-Aty H, Taylor A, Schulz-Menger J, Messroghli D, Dietz R. The salvaged area at risk in reperfused acute myocardial infarction as visualized by cardiovascular magnetic resonance. J Am Coll Cardiol 2008;51:1581–7.
40. Cury RC, Shash K, Nagurney JT, et al. Cardiac magnetic resonance with T2-weighted imaging improves detection of patients with acute coronary syndrome in the emergency department. Circulation 2008; 118:837–44.
41. Kellman P, Aletras AH, Mancini C, McVeigh ER, Arai AE. T2-prepared SSFP improves diagnostic confidence in edema imaging in acute myocardial infarction compared to turbo spin echo. Magn Reson Med 2007;57:891–7.
42. Aletras AH, Kellman P, Derbyshire JA, Arai AE. ACUT2E TSE-SSFP: a hybrid method for T2-weighted imaging of edema in the heart. Magn Reson Med 2008;59:229–35.
43. Weinsaft JW, Kim HW, Shah DJ, et al. Detection of left ventricular thrombus by delayed-enhancement cardiovascular magnetic resonance prevalence and markers in patients with systolic dysfunction. J Am Coll Cardiol 2008;52:148–57.
44. Shapiro MD, Guarraia DL, Moloo J, Cury RC. Evaluation of acute coronary syndromes by cardiac magnetic resonance imaging. Top Magn Reson Imaging 2008;19:25–32.
45. Nandalur KR, Dwamena BA, Choudhri AF, Nandalur MR, Carlos RC. Diagnostic performance of stress cardiac magnetic resonance imaging in the detection of coronary artery disease: a meta-analysis. J Am Coll Cardiol 2007;50:1343–53.
46. Cheng AS, Pegg TJ, Karamitsos TD, et al. Cardiovascular magnetic resonance perfusion imaging at 3-Tesla for the detection of coronary artery disease: a comparison with 1.5-Tesla. J Am Coll Cardiol 2007;49:2440–9.
47. Nagel E, Klein C, Paetsch I, et al. Magnetic resonance perfusion measurements for the noninvasive detection of coronary artery disease. Circulation 2003;108:432–7.
48. Plein S, Radjenovic A, Ridgway JP, et al. Coronary artery disease: myocardial perfusion MR imaging with sensitivity encoding versus conventional angiography. Radiology 2005;235:423–30.
49. Schwitter J, Wacker CM, van Rossum AC, et al. MR-IMPACT: comparison of perfusion-cardiac magnetic resonance with single-photon emission computed tomography for the detection of coronary artery disease in a multicentre, multivendor, randomized trial. Eur Heart J 2008;29:480–9.
50. Karamitsos TD, Arnold JR, Pegg TJ, et al. Tolerance and safety of adenosine stress perfusion cardiovascular magnetic resonance imaging in patients with severe coronary artery disease. Int J Cardiovasc Imaging 2009;25:277–83.
51. Schwitter J, Wacker CM, van Rossum AC, et al. MR-IMPACT: comparison of perfusion-cardiac magnetic resonance with single-photon emission computed tomography for the detection of coronary artery disease in a multicentre, multivendor, randomized trial. Eur Heart J 2008;29:480–9.
52. Wahl A, Paetsch I, Gollesch A, et al. Safety and feasibility of high-dose dobutamine-atropine stress cardiovascular magnetic resonance for diagnosis of myocardial ischaemia: experience in 1000 consecutive cases. Eur Heart J 2004;25:1230–6.
53. Mandapaka S, Hundley WG. Dobutamine cardiovascular magnetic resonance: a review. J Magn Reson Imaging 2006;24:499–512.
54. Hundley WG, Hamilton CA, Thomas MS, et al. Utility of fast cine magnetic resonance imaging and display for the detection of myocardial ischemia in patients not well suited for second harmonic stress echocardiography. Circulation 1999;100:1697–702.
55. Bluemke DA, Achenbach S, Budoff M, et al. Noninvasive coronary artery imaging: magnetic resonance angiography and multidetector computed tomography angiography: a scientific statement from the American Heart Association Committee on Cardiovascular Imaging and Intervention of the Council on Cardiovascular Radiology and Intervention, and the Councils on Clinical Cardiology and Cardiovascular Disease in the Young. Circulation 2008;118:586–606.
56. McCrohon JA, Moon JC, Prasad SK, et al. Differentiation of heart failure related to dilated cardiomyopathy and coronary artery disease using gadolinium-enhanced cardiovascular magnetic resonance. Circulation 2003;108:54–9.
57. Casolo G, Minneci S, Manta R, et al. Identification of the ischemic etiology of heart failure by cardiovascular magnetic resonance imaging: diagnostic accuracy of late gadolinium enhancement. Am Heart J 2006;151:101–8.
58. Soriano CJ, Ridocci F, Estornell J, Jimenez J, Martinez V, De Velasco JA. Noninvasive diagnosis of coronary artery disease in patients with heart failure and systolic dysfunction of uncertain

etiology, using late gadolinium-enhanced cardiovascular magnetic resonance. J Am Coll Cardiol 2005;45:743–8.
59. Roberts WC, Siegel RJ, McManus BM. Idiopathic dilated cardiomyopathy: analysis of 152 necropsy patients. Am J Cardiol 1987;60:1340–55.
60. Bogun FM, Desjardins B, Good E, et al. Delayed-enhanced magnetic resonance imaging in nonischemic cardiomyopathy: utility for identifying the ventricular arrhythmia substrate. J Am Coll Cardiol 2009;53:1138–45.
61. Friedrich MG, Strohm O, Schulz-Menger J, Marciniak H, Luft FC, Dietz R. Contrast media-enhanced magnetic resonance imaging visualizes myocardial changes in the course of viral myocarditis. Circulation 1998;97:1802–9.
62. Abdel-Aty H, Boye P, Zagrosek A, et al. Diagnostic performance of cardiovascular magnetic resonance in patients with suspected acute myocarditis: comparison of different approaches. J Am Coll Cardiol 2005;45:1815–22.
63. Mahrholdt H, Goedecke C, Wagner A, et al. Cardiovascular magnetic resonance assessment of human myocarditis: a comparison to histology and molecular pathology. Circulation 2004;109:1250–8.
64. Mahrholdt H, Wagner A, Deluigi CC, et al. Presentation, patterns of myocardial damage, and clinical course of viral myocarditis. Circulation 2006;114:1581–90.
65. De Cobelli F, Pieroni M, Esposito A, et al. Delayed gadolinium-enhanced cardiac magnetic resonance in patients with chronic myocarditis presenting with heart failure or recurrent arrhythmias. J Am Coll Cardiol 2006;47:1649–54.
66. Pons-Llado G, Carreras F, Borras X, Palmer J, Llauger J, Bayes de Luna A. Comparison of morphologic assessment of hypertrophic cardiomyopathy by magnetic resonance versus echocardiographic imaging. Am J Cardiol 1997;79:1651–6.
67. Rickers C, Wilke NM, Jerosch-Herold M, et al. Utility of cardiac magnetic resonance imaging in the diagnosis of hypertrophic cardiomyopathy. Circulation 2005;112:855–61.
68. Olivotto I, Maron MS, Autore C, et al. Assessment and significance of left ventricular mass by cardiovascular magnetic resonance in hypertrophic cardiomyopathy. J Am Coll Cardiol 2008;52:559–66.
69. Moon JC, Fisher NG, McKenna WJ, Pennell DJ. Detection of apical hypertrophic cardiomyopathy by cardiovascular magnetic resonance in patients with non-diagnostic echocardiography. Heart 2004;90:645–9.
70. Spirito P, Bellone P, Harris KM, Bernabo P, Bruzzi P, Maron BJ. Magnitude of left ventricular hypertrophy and risk of sudden death in hypertrophic cardiomyopathy. N Engl J Med 2000;342:1778–85.
71. Kwon DH, Setser RM, Thamilarasan M, et al. Abnormal papillary muscle morphology is independently associated with increased left ventricular outflow tract obstruction in hypertrophic cardiomyopathy. Heart 2008;94:1295–301.
72. Rudolph A, Abdel-Aty H, Bohl S, et al. Noninvasive detection of fibrosis applying contrast-enhanced cardiac magnetic resonance in different forms of left ventricular hypertrophy relation to remodeling. J Am Coll Cardiol 2009;53:284–91.
73. Yamada M, Teraoka K, Kawade M, Hirano M, Yamashina A. Frequency and distribution of late gadolinium enhancement in magnetic resonance imaging of patients with apical hypertrophic cardiomyopathy and patients with asymmetrical hypertrophic cardiomyopathy: a comparative study. Int J Cardiovasc Imaging 2009;25 Suppl 1:131–8.
74. Bogaert J, Goldstein M, Tannouri F, Golzarian J, Dymarkowski S. Original report. Late myocardial enhancement in hypertrophic cardiomyopathy with contrast-enhanced MR imaging. AJR Am J Roentgenol 2003;180:981–5.
75. Moon JC, Reed E, Sheppard MN, et al. The histologic basis of late gadolinium enhancement cardiovascular magnetic resonance in hypertrophic cardiomyopathy. J Am Coll Cardiol 2004;43:2260–4.
76. Moon JC, McKenna WJ, McCrohon JA, Elliott PM, Smith GC, Pennell DJ. Toward clinical risk assessment in hypertrophic cardiomyopathy with gadolinium cardiovascular magnetic resonance. J Am Coll Cardiol 2003;41:1561–7.
77. Choudhury L, Mahrholdt H, Wagner A, et al. Myocardial scarring in asymptomatic or mildly symptomatic patients with hypertrophic cardiomyopathy. J Am Coll Cardiol 2002;40:2156–64.
78. Petersen SE, Jerosch-Herold M, Hudsmith LE, et al. Evidence for microvascular dysfunction in hypertrophic cardiomyopathy: new insights from multiparametric magnetic resonance imaging. Circulation 2007;115:2418–25.
79. Maron MS, Finley JJ, Bos JM, et al. Prevalence, clinical significance, and natural history of left ventricular apical aneurysms in hypertrophic cardiomyopathy. Circulation 2008;118:1541–9.
80. Ferrari VA, Scott CH, Basso C. Arrhythmogenic right ventricular dysplasia/cardiomyopathy. Curr Cardiol Rep 2005;7:70–5.
81. Corrado D, Basso C, Thiene G, et al. Spectrum of clinicopathologic manifestations of arrhythmogenic right ventricular cardiomyopathy/dysplasia: a multicenter study. J Am Coll Cardiol 1997;30:1512–20.
82. Sen-Chowdhry S, Syrris P, Prasad SK, et al. Left-dominant arrhythmogenic cardiomyopathy: an under-recognized clinical entity. J Am Coll Cardiol 2008;52:2175–87.
83. Jain A, Tandri H, Calkins H, Bluemke DA. Role of cardiovascular magnetic resonance imaging in arrhythmogenic right ventricular dysplasia. J Cardiovasc Magn Reson 2008;10:32.
84. Tandri H, Bomma C, Calkins H, Bluemke DA. Magnetic resonance and computed tomography imaging of arrhythmogenic right ventricular dysplasia. J Magn Reson Imaging 2004;19:848–58.
85. McKenna WJ, Thiene G, Nava A, et al. Diagnosis of arrhythmogenic right ventricular dysplasia/cardiomyopathy. Task Force of the Working Group Myocardial and Pericardial Disease of the European Society of Cardiology and of the Scientific Council on Cardiomyopathies of the International Society and Federation of Cardiology. Br Heart J 1994;71:215–8.
86. Tandri H, Saranathan M, Rodriguez ER, et al. Noninvasive detection of myocardial fibrosis in arrhythmogenic right ventricular cardiomyopathy using delayed-enhancement magnetic resonance imaging. J Am Coll Cardiol 2005;45:98–103.
87. Hunold P, Wieneke H, Bruder O, et al. Late enhancement: a new feature in MRI of arrhythmogenic right ventricular cardiomyopathy? J Cardiovasc Magn Reson 2005;7:649–55.
88. Tandri H, Castillo E, Ferrari VA, et al. Magnetic resonance imaging of arrhythmogenic right ventricular dysplasia: sensitivity, specificity, and observer variability of fat detection versus functional analysis of the right ventricle. J Am Coll Cardiol 2006;48:2277–84.
89. Sen-Chowdhry S, Prasad SK, Syrris P, et al. Cardiovascular magnetic resonance in arrhythmogenic right ventricular cardiomyopathy revisited: comparison with task force criteria and genotype. J Am Coll Cardiol 2006;48:2132–40.
90. Borgna-Pignatti C, Cappellini MD, De Stefano P, et al. Survival and complications in thalassemia. Ann N Y Acad Sci 2005;1054:40–7.
91. Anderson LJ, Holden S, Davis B, et al. Cardiovascular T2-star (T2*) magnetic resonance for the early diagnosis of myocardial iron overload. Eur Heart J 2001;22:2171–9.
92. Westwood M, Anderson LJ, Firmin DN, et al. A single breath-hold multiecho T2* cardiovascular magnetic resonance technique for diagnosis of myocardial iron overload. J Magn Reson Imaging 2003;18:33–9.
93. Tanner MA, Galanello R, Dessi C, et al. A randomized, placebo-controlled, double-blind trial of the effect of combined therapy with deferoxamine and deferiprone on myocardial iron in thalassemia major using cardiovascular magnetic resonance. Circulation 2007;115:1876–84.
94. Anderson LJ, Wonke B, Prescott E, Holden S, Walker JM, Pennell DJ. Comparison of effects of oral deferiprone and subcutaneous desferrioxamine on myocardial iron concentrations and ventricular function in beta-thalassaemia. Lancet 2002;360:516–20.
95. Selvanayagam JB, Hawkins PN, Paul B, Myerson SG, Neubauer S. Evaluation and management of the cardiac amyloidosis. J Am Coll Cardiol 2007;50:2101–10.
96. Maceira AM, Joshi J, Prasad SK, et al. Cardiovascular magnetic resonance in cardiac amyloidosis. Circulation 2005;111:186–93.
97. Cheng AS, Banning AP, Mitchell AR, Neubauer S, Selvanayagam JB. Cardiac changes in systemic amyloidosis: visualisation by magnetic resonance imaging. Int J Cardiol 2006;113:E21–3.
98. Vogelsberg H, Mahrholdt H, Deluigi CC, et al. Cardiovascular magnetic resonance in clinically suspected cardiac amyloidosis: noninvasive imaging compared to endomyocardial biopsy. J Am Coll Cardiol 2008;51:1022–30.
99. Sharma OP, Maheshwari A, Thaker K. Myocardial sarcoidosis. Chest 1993;103:253–8.

100. Silverman KJ, Hutchins GM, Bulkley BH. Cardiac sarcoid a clinicopathologic study of 84 unselected patients with systemic sarcoidosis. Circulation 1978;58:1204–11.
101. Doughan AR, Williams BR. Cardiac sarcoidosis. Heart 2006;92: 282–8.
102. Roberts WC, McAllister HA Jr., Ferrans VJ. Sarcoidosis of the heart. A clinicopathologic study of 35 necropsy patients (group 1) and review of 78 previously described necropsy patients (group 11). Am J Med 1977;63:86–108.
103. Serra JJ, Monte GU, Mello ES, et al. Images in cardiovascular medicine. Cardiac sarcoidosis evaluated by delayed-enhanced magnetic resonance imaging. Circulation 2003;107:e188–9.
104. Smedema JP, Snoep G, van Kroonenburgh MP, et al. Evaluation of the accuracy of gadolinium-enhanced cardiovascular magnetic resonance in the diagnosis of cardiac sarcoidosis. J Am Coll Cardiol 2005;45:1683–90.
105. Smedema JP, Snoep G, van Kroonenburgh MP, et al. The additional value of gadolinium-enhanced MRI to standard assessment for cardiac involvement in patients with pulmonary sarcoidosis. Chest 2005;128:1629–37.
106. Yared K, Johri AM, Soni AV, et al. Cardiac sarcoidosis imitating arrhythmogenic right ventricular dysplasia. Circulation 2008;118: e113–5.
107. Schulz-Menger J, Wassmuth R, Abdel-Aty H, et al. Patterns of myocardial inflammation and scarring in sarcoidosis as assessed by cardiovascular magnetic resonance. Heart 2006;92:399–400.
108. Vignaux O, Dhote R, Duboc D, et al. Detection of myocardial involvement in patients with sarcoidosis applying T2-weighted, contrast-enhanced, and cine magnetic resonance imaging: initial results of a prospective study. J Comput Assist Tomogr 2002;26: 762–7.
109. Clarke JT. Narrative review: Fabry disease. Ann Intern Med 2007; 146:425–33.
110. Moon JC, Sheppard M, Reed E, Lee P, Elliott PM, Pennell DJ. The histological basis of late gadolinium enhancement cardiovascular magnetic resonance in a patient with Anderson-Fabry disease. J Cardiovasc Magn Reson 2006;8:479–82.
111. Sachdev B, Takenaka T, Teraguchi H, et al. Prevalence of Anderson-Fabry disease in male patients with late onset hypertrophic cardiomyopathy. Circulation 2002;105:1407–11.
112. Frustaci A, Chimenti C, Ricci R, et al. Improvement in cardiac function in the cardiac variant of Fabry's disease with galactose-infusion therapy. N Engl J Med 2001;345:25–32.
113. Hughes DA, Elliott PM, Shah J, et al. Effects of enzyme replacement therapy on the cardiomyopathy of Anderson-Fabry disease: a randomised, double-blind, placebo-controlled clinical trial of agalsidase alfa. Heart 2008;94:153–8.
114. Weidemann F, Niemann M, Breunig F, et al. Long-term effects of enzyme replacement therapy on Fabry cardiomyopathy: evidence for a better outcome with early treatment. Circulation 2009;119:524–9.
115. Masui T, Finck S, Higgins CB. Constrictive pericarditis and restrictive cardiomyopathy: evaluation with MR imaging. Radiology 1992; 182:369–73.
116. Francone M, Dymarkowski S, Kalantzi M, Rademakers FE, Bogaert J. Assessment of ventricular coupling with real-time cine MRI and its value to differentiate constrictive pericarditis from restrictive cardiomyopathy. Eur Radiol 2006;16:944–51.
117. McCrohon JA, Richmond DR, Pennell DJ, Mohiaddin RH. Images in cardiovascular medicine. Isolated noncompaction of the myocardium: a rarity or missed diagnosis? Circulation 2002;106:e22–3.
118. Petersen SE, Selvanayagam JB, Wiesmann F, et al. Left ventricular non-compaction: insights from cardiovascular magnetic resonance imaging. J Am Coll Cardiol 2005;46:101–5.
119. Rochitte CE, Oliveira PF, Andrade JM, et al. Myocardial delayed enhancement by magnetic resonance imaging in patients with Chagas' disease: a marker of disease severity. J Am Coll Cardiol 2005;46:1553–8.
120. Rochitte CE, Nacif MS, de Oliveira AC Jr., et al. Cardiac magnetic resonance in Chagas' disease. Artif Organs 2007;31:259–67.
121. Wassmuth R, Gobel U, Natusch A, et al. Cardiovascular magnetic resonance imaging detects cardiac involvement in Churg-Strauss syndrome. J Card Fail 2008;14:856–60.
122. Genee O, Fichet J, Alison D. Images in cardiovascular medicine: cardiac magnetic resonance imaging and eosinophilic endomyocardial fibrosis. Circulation 2008;118:e710–1.
123. Haghi D, Fluechter S, Suselbeck T, Kaden JJ, Borggrefe M, Papavassiliu T. Cardiovascular magnetic resonance findings in typical versus atypical forms of the acute apical ballooning syndrome (Takotsubo cardiomyopathy). Int J Cardiol 2007;120:205–11.
124. Karamitsos TD, Bull S, Spyrou N, Neubauer S, Selvanayagam JB. Tako-tsubo cardiomyopathy presenting with features of left ventricular non-compaction. Int J Cardiol 2008;128:e34–6.
125. Abdel-Aty H, Cocker M, Friedrich MG. Myocardial edema is a feature of Tako-Tsubo cardiomyopathy and is related to the severity of systolic dysfunction: insights from T2-weighted cardiovascular magnetic resonance. Int J Cardiol 2009;132:291–3.
126. Karamitsos TD, Bull S, Francis JM, et al. Massive melanotic myocardial metastasis characterized by multiple cardiac imaging modalities. Int J Cardiol 2009 Jan 29 [E-pub ahead of print].
127. Syed IS, Feng D, Harris SR, et al. MR imaging of cardiac masses. Magn Reson Imaging Clin N Am 2008;16:137–64, vii.
128. Gutierrez FR, Ho ML, Siegel MJ. Practical applications of magnetic resonance in congenital heart disease. Magn Reson Imaging Clin N Am 2008;16:403–35.
129. Bax JJ, Abraham T, Barold SS, et al. Cardiac resynchronization therapy: part 1—issues before device implantation. J Am Coll Cardiol 2005;46:2153–67.
130. Chung ES, Leon AR, Tavazzi L, et al. Results of the Predictors of Response to CRT (PROSPECT) trial. Circulation 2008;117:2608–16.
131. Helm RH, Lardo AC. Cardiac magnetic resonance assessment of mechanical dyssynchrony. Curr Opin Cardiol 2008;23:440–6.
132. Chalil S, Stegemann B, Muhyaldeen S, et al. Intraventricular dyssynchrony predicts mortality and morbidity after cardiac resynchronization therapy: a study using cardiovascular magnetic resonance tissue synchronization imaging. J Am Coll Cardiol 2007;50: 243–52.
133. White JA, Yee R, Yuan X, et al. Delayed enhancement magnetic resonance imaging predicts response to cardiac resynchronization therapy in patients with intraventricular dyssynchrony. J Am Coll Cardiol 2006;48:1953–60.
134. Ypenburg C, Schalij MJ, Bleeker GB, et al. Impact of viability and scar tissue on response to cardiac resynchronization therapy in ischaemic heart failure patients. Eur Heart J 2007;28:33–41.
135. Reuter S, Garrigue S, Barold SS, et al. Comparison of characteristics in responders versus nonresponders with biventricular pacing for drug-resistant congestive heart failure. Am J Cardiol 2002;89:346–50.
136. Bleeker GB, Kaandorp TA, Lamb HJ, et al. Effect of posterolateral scar tissue on clinical and echocardiographic improvement after cardiac resynchronization therapy. Circulation 2006;113:969–76.
137. Chiribiri A, Kelle S, Gotze S, et al. Visualization of the cardiac venous system using cardiac magnetic resonance. Am J Cardiol 2008;101:407–12.
138. Beeres SL, Bengel FM, Bartunek J, et al. Role of imaging in cardiac stem cell therapy. J Am Coll Cardiol 2007;49:1137–48.
139. Ly HQ, Frangioni JV, Hajjar RJ. Imaging in cardiac cell-based therapy: in vivo tracking of the biological fate of therapeutic cells. Nat Clin Pract Cardiovasc Med 2008;5 Suppl 2:S96–102.
140. Bello D, Fieno DS, Kim RJ, et al. Infarct morphology identifies patients with substrate for sustained ventricular tachycardia. J Am Coll Cardiol 2005;45:1104–8.
141. Yan AT, Shayne AJ, Brown KA, et al. Characterization of the peri-infarct zone by contrast-enhanced cardiac magnetic resonance imaging is a powerful predictor of post-myocardial infarction mortality. Circulation 2006;114:32–9.
142. Schmidt A, Azevedo CF, Cheng A, et al. Infarct tissue heterogeneity by magnetic resonance imaging identifies enhanced cardiac arrhythmia susceptibility in patients with left ventricular dysfunction. Circulation 2007;115:2006–14.
143. Larose E, Ganz P, Reynolds HG, et al. Right ventricular dysfunction assessed by cardiovascular magnetic resonance imaging predicts poor prognosis late after myocardial infarction. J Am Coll Cardiol 2007; 49:855–62.
144. Kwong RY, Chan AK, Brown KA, et al. Impact of unrecognized myocardial scar detected by cardiac magnetic resonance imaging on event-free survival in patients presenting with signs or symptoms of coronary artery disease. Circulation 2006;113:2733–43.

145. Jahnke C, Nagel E, Gebker R, et al. Prognostic value of cardiac magnetic resonance stress tests: adenosine stress perfusion and dobutamine stress wall motion imaging. Circulation 2007;115:1769–76.
146. Dall'Armellina E, Morgan TM, Mandapaka S, et al. Prediction of cardiac events in patients with reduced left ventricular ejection fraction with dobutamine cardiovascular magnetic resonance assessment of wall motion score index. J Am Coll Cardiol 2008;52:279–86.
147. Bodi V, Sanchis J, Lopez-Lereu MP, et al. Prognostic value of dipyridamole stress cardiovascular magnetic resonance imaging in patients with known or suspected coronary artery disease. J Am Coll Cardiol 2007;50:1174–9.
148. Assomull RG, Prasad SK, Lyne J, et al. Cardiovascular magnetic resonance, fibrosis, and prognosis in dilated cardiomyopathy. J Am Coll Cardiol 2006;48:1977–85.
149. Wu KC, Weiss RG, Thiemann DR, et al. Late gadolinium enhancement by cardiovascular magnetic resonance heralds an adverse prognosis in nonischemic cardiomyopathy. J Am Coll Cardiol 2008;51:2414–21.
150. Nazarian S, Bluemke DA, Lardo AC, et al. Magnetic resonance assessment of the substrate for inducible ventricular tachycardia in nonischemic cardiomyopathy. Circulation 2005;112:2821–5.
151. Adabag AS, Maron BJ, Appelbaum E, et al. Occurrence and frequency of arrhythmias in hypertrophic cardiomyopathy in relation to delayed enhancement on cardiovascular magnetic resonance. J Am Coll Cardiol 2008;51:1369–74.
152. Kwon DH, Setser RM, Popovic ZB, et al. Association of myocardial fibrosis, electrocardiography and ventricular tachyarrhythmia in hypertrophic cardiomyopathy: a delayed contrast enhanced MRI study. Int J Cardiovasc Imaging 2008;24:617–25.
153. Maceira AM, Prasad SK, Hawkins PN, Roughton M, Pennell DJ. Cardiovascular magnetic resonance and prognosis in cardiac amyloidosis. J Cardiovasc Magn Reson 2008;10:54.
154. Ruberg FL, Appelbaum E, Davidoff R, et al. Diagnostic and prognostic utility of cardiovascular magnetic resonance imaging in light-chain cardiac amyloidosis. Am J Cardiol 2009;103:544–9.
155. Kirk P, Roughton M, Porter JB, et al. Cardiac T2* magnetic resonance for prediction of cardiac complications in thalassemia major. J Cardiovasc Magn Reson 2009;11 Suppl 1:O2.
156. Hendel RC, Patel MR, Kramer CM, et al. ACCF/ACR/SCCT/SCMR/ASNC/NASCI/SCAI/SIR 2006 appropriateness criteria for cardiac computed tomography and cardiac magnetic resonance imaging: a report of the American College of Cardiology Foundation Quality Strategic Directions Committee Appropriateness Criteria Working Group, American College of Radiology, Society of Cardiovascular Computed Tomography, Society for Cardiovascular Magnetic Resonance, American Society of Nuclear Cardiology, North American Society for Cardiac Imaging, Society for Cardiovascular Angiography and Interventions, and Society of Interventional Radiology. J Am Coll Cardiol 2006;48:1475–97.
157. Iles L, Pfluger H, Phrommintikul A, et al. Evaluation of diffuse myocardial fibrosis in heart failure with cardiac magnetic resonance contrast-enhanced T1 mapping. J Am Coll Cardiol 2008;52:1574–80.
158. Ratnayaka K, Faranesh AZ, Guttman MA, Kocaturk O, Saikus CE, Lederman RJ. Interventional cardiovascular magnetic resonance: still tantalizing. J Cardiovasc Magn Reson 2008;10:62.
159. Lurz P, Coats L, Khambadkone S, et al. Percutaneous pulmonary valve implantation: impact of evolving technology and learning curve on clinical outcome. Circulation 2008;117:1964–72.
160. Razavi R, Hill DL, Keevil SF, et al. Cardiac catheterisation guided by MRI in children and adults with congenital heart disease. Lancet 2003;362:1877–82.
161. Neubauer S. The failing heart—an engine out of fuel. N Engl J Med 2007;356:1140–51.

Key Words: left ventricular dysfunction ■ heart failure ■ ischemia ■ diagnosis ■ therapy ■ prognosis ■ cardiovascular magnetic resonance imaging.

APPENDIX

For accompanying Online Videos 1 and 2 and their legends, please see the online version of this article